

Controlled tissue emulsification produced by high intensity focused ultrasound shock waves and millisecond boiling

Tatiana D. Khokhlova^{a)}

Center for Industrial and Medical Ultrasound, Applied Physics Laboratory, University of Washington,
1013 NE 40th Street, Seattle, Washington 98105

Michael S. Canney

Inserm, U1032, 151 Cours Albert Thomas, Lyon, F-69003, France

Vera A. Khokhlova^{b)} and Oleg A. Sapozhnikov^{b)}

Department of Acoustics, Physics Faculty, Moscow State University, Leninskie Gory, Moscow 119991, Russia

Lawrence A. Crum and Michael R. Bailey

Center for Industrial and Medical Ultrasound, Applied Physics Laboratory, University of Washington,
1013 NE 40th Street, Seattle Washington 98105

(Received 17 December 2010; revised 18 May 2011; accepted 19 May 2011)

In high intensity focused ultrasound (HIFU) applications, tissue may be thermally necrosed by heating, emulsified by cavitation, or, as was recently discovered, emulsified using repetitive millisecond boiling caused by shock wave heating. Here, this last approach was further investigated. Experiments were performed in transparent gels and *ex vivo* bovine heart tissue using 1, 2, and 3 MHz focused transducers and different pulsing schemes in which the pressure, duty factor, and pulse duration were varied. A previously developed derating procedure to determine *in situ* shock amplitudes and the time-to-boil was refined. Treatments were monitored using B-mode ultrasound. Both inertial cavitation and boiling were observed during exposures, but emulsification occurred only when shocks and boiling were present. Emulsified lesions without thermal denaturation were produced with shock amplitudes sufficient to induce boiling in less than 20 ms, duty factors of less than 0.02, and pulse lengths shorter than 30 ms. Higher duty factors or longer pulses produced varying degrees of thermal denaturation combined with mechanical emulsification. Larger lesions were obtained using lower ultrasound frequencies. The results show that shock wave heating and millisecond boiling is an effective and reliable way to emulsify tissue while monitoring the treatment with ultrasound. © 2011 Acoustical Society of America.

[DOI: 10.1121/1.3626152]

PACS number(s): 43.80.Sh, 43.25.Cb [CCC]

Pages: 3498–3510

I. INTRODUCTION

Transcutaneous high intensity focused ultrasound (HIFU) is an emerging medical technology used to necrotize benign and malignant tumors in tissue.^{1,2} Most HIFU treatments are designed to utilize thermal effects resulting from absorption of ultrasound by tissue to create a thermally coagulated treatment volume. Alternatively, mechanical effects generated by HIFU-induced bubbles may be used to disrupt tissue,³ and leave a fluid-filled treatment volume^{4,5} or be used to cut through tissue such as the heart septum.⁶ Mechanical effects are typically induced by operating HIFU sources using sequences of pulses rather than in a continuous wave (CW) mode to minimize thermal effects and to maximize the effects of bubble activity.

A type of pulsing protocol designed to induce mechanical disruption of tissue has been demonstrated and termed “histotripsy.”⁷ Lower frequency HIFU sources (0.75–1 MHz) are operated at low duty factors (<0.01) and high outputs to generate large peak negative pressures (>20 MPa) in the focal region.⁴ Thousands to tens of thousands of pulses, each only several microseconds in duration, are delivered to form one void. Tissue emulsification produced using this method is attributed to the action of a cavitation cloud that forms at the focus of the transducer. The lesion morphology that has been observed with histotripsy exposures is significantly different than that observed with conventional, CW HIFU exposures, and consists of well-demarcated regions of fluid-like homogenized tissue with little evidence of either thermal denaturation or remaining cellular integrity.^{4,8}

Although the present histotripsy techniques have been shown to be promising, there are a number of challenges associated with their practical application, mostly related to the stochastic nature of cavitation. The time to initiate bubble clouds in tissue is not always predictable and repeatable, and cavitation activity can stop unexpectedly in the course of the treatment, resulting in extinction of the bubble cloud.⁸

^{a)}Author to whom correspondence should be addressed. Electronic mail: tanyak@apl.washington.edu

^{b)}Also at: Center for Industrial and Medical Ultrasound, Applied Physics Laboratory, University of Washington, 1013 NE 40th Street, Seattle Washington 98105.

Designing newer approaches that result in reliable and reproducible mechanical tissue damage is therefore of considerable interest.

Recently, it was proposed that tissue emulsification can also be produced by using millisecond instead of microsecond duration HIFU pulses and boiling as opposed to cavitation.⁹ Our previous studies showed that absorption at shocks formed at the focus of a HIFU beam can lead to temperatures of over 100°C and localized boiling in only several milliseconds.¹⁰ The formation of shocks and corresponding enhanced heating occurs in a region of only several hundred microns or less in width,^{10,11} thus the heated (likely super heated)^{12,13} and potentially necrotized region is small compared to the volume occupied by the millimeter-sized boiling bubble created. If the HIFU pulse length is slightly longer than the time-to-boil (discussed in Sec. II E), then the thermal injury induced is negligible compared to the mechanical injury caused by the exploding bubble and its further interaction with shocks. A corresponding pulsing protocol (2 MHz frequency, 70 MPa shock amplitude at the focus, 10 ms pulse duration, 0.01 duty factor) was found to produce emulsification and no observable thermal necrosis in *ex vivo* bovine liver and heart tissue.⁹

In this study, the physical mechanisms of tissue damage that involve shock wave heating and millisecond boiling were further investigated. Experiments were performed in transparent gels and *ex vivo* bovine heart and liver tissue. Multiple output parameters including pulse length, duty factor, focal pressures, and frequency were varied to determine the parameter space around millisecond pulses relative to the transition from emulsification to coagulation. HIFU-induced bubbles were observed and inertial cavitation was distinguished from boiling in pulse sequences by monitoring fluctuations in voltage at the HIFU source, by using B-mode ultrasound imaging, and by recording images using a high-speed camera (in experiments using transparent, tissue-mimicking phantoms). The relative roles of boiling and cavitation were correlated to the bioeffects produced. The time-to-boil was predicted using weak shock theory, confirmed in experiments, and then used to define pulse lengths and duty factors to create predictable emulsified tissue volumes. After exposures, tissue samples were sectioned and gross lesion morphologies were categorized according to the relative thermal or mechanical effects observed.

II. MATERIALS AND METHODS

HIFU exposures were performed in transparent gel phantoms and in *ex vivo* tissue samples. Acoustic characterization of *in situ* HIFU fields was performed using the combined measurement and modeling approach developed in our previously published studies and is summarized in Sec. II C.^{10,11,14} The following notation is used throughout the paper for the exposure parameters: p^+ is peak positive pressure, p^- is peak negative pressure in the focal waveform, p_0 is pressure amplitude at the surface of the transducer, used in the modeling, that corresponds to a given electric power into the transducer W_{el} in the measurements,¹¹ I_L is peak focal intensity assuming linear acoustic propagation, t_{pulse} is pulse

duration, t_b is time-to-boil, and DF is the duty factor, which is the ratio between the pulse length and the period between the pulses.

A. Experimental arrangement

A diagram of the experimental arrangement is shown in Fig. 1. The experiments were performed in an acrylic water tank at room temperature (20°C). The tank was filled with purified water that was degassed using a multiple pinhole degasser to 25% of saturation, as measured by a dissolved oxygen meter (WTW Oxi 330i, Weilheim, Germany). The HIFU source used in the majority of the experiments was a single-element, air-backed, custom-built piezoceramic transducer of 2.158 MHz frequency, 44 mm aperture, and focal length (f -number = 1). The transducer was driven by a function generator (Agilent 33250A, Agilent, Palo Alto, CA) and a rf amplifier (300W, ENI A-300, ENI, Rochester, NY). In addition, two other HIFU transducers with frequencies of 1.1 and 3.4 MHz were used in a small set of experiments to investigate the effect of frequency on the resulting tissue damage. The 1.1 MHz source (also 44 mm aperture and focal length) was driven by a separate rf amplifier (1000W, RFG-1000, JJ&A Instruments, Duvall, WA). The 3.4 MHz transducer (H-102 model, outer aperture 64 mm and focal length 62.6 mm, Sonic Concepts, Bothell, WA) was driven with the same electronics as the 2 MHz source. A timing board (NI 6608, National Instruments, Austin, TX) was used to trigger the function generator for various pulsing protocols and was controlled using a custom Labview program (National Instruments, Austin, TX). The HIFU source was attached to a three-axis positioning system (Velmex Inc., Bloomfield,

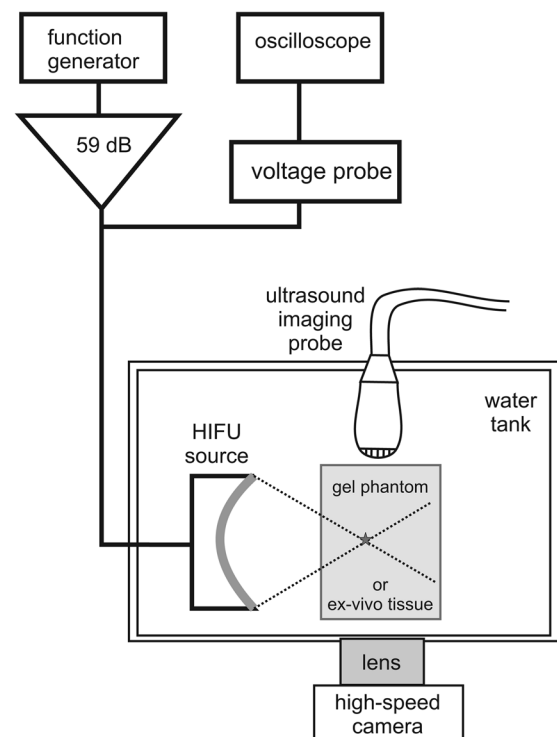


FIG. 1. A diagram of the experimental setup that was used to produce HIFU lesions and monitor cavitation and boiling bubbles in transparent polyacrylamide gel and *ex vivo* tissue.

NY) to align the focus with the desired position within the exposure sample.

B-mode ultrasound imaging was performed during experiments using an HDI-1000 scanner with a CL10-5 scanhead (Philips Medical Systems, Bothell, WA). The excitation voltage at the HIFU source was monitored using a 10x Lecroy high-voltage probe in parallel with the HIFU transducer. The voltage was recorded using a digital oscilloscope (LT344, Lecroy, Chestnut Ridge, NY) and fluctuations in the rms voltage were used to indicate the onset of boiling at the focus.^{10,15–17} The fluctuations in the voltage are caused by transduction of ultrasound energy that is backscattered from boiling bubbles at the focus. A high-speed camera (Fastrax APX-RS, Photron, San Diego, CA) was used simultaneously with the ultrasound imaging system for viewing heating effects and bubbles in transparent gel phantoms. The camera was operated at a pixel resolution of 1024×1024 and a Nikon 105 mm lens (Nikon, Melville, NY, USA) was used with a bellows extension to obtain a field of view of $10 \text{ mm} \times 10 \text{ mm}$ ($10 \mu\text{m}/\text{pixel}$). The frames were recorded at 20 000 frames per second (fps) with a $4 \mu\text{s}$ shutter speed. All the images presented herein were backlit.

B. Preparation of transparent gel phantoms and tissue samples

Gel phantoms were prepared using polyacrylamide with 7% bovine serum albumin (BSA).¹⁸ These gels are optically transparent and have similar acoustic properties to tissue except for the attenuation coefficient, which is about three times lower than most tissues ($0.15 \text{ dB}/\text{cm}/\text{MHz}$). Localized heating of the gels causes the BSA to denature and form an opaque region above temperatures of $\sim 60^\circ\text{C}$ that can be visualized optically. To prepare the samples, the liquid mixture of gel constituents was degassed for 1 h in a desiccant chamber, then poured into a custom mold and polymerized.¹⁰ A 1 mm needle was attached to the mold and placed within the gel for alignment purposes.

Tissue samples were prepared from bovine heart or liver tissue. The tissue was obtained from an abattoir on the same day as experiments and stored in phosphate buffered saline and on ice until experiments were performed. The tissue was cut into samples to fit in a custom-designed tissue holder (8 cm wide by 8 cm tall by 2.7 cm deep) and was degassed for 1 h in a desiccant chamber immediately prior to experiments. The heart tissue samples were oriented so that the ultrasound was incident perpendicularly to the muscle fibers. For positioning the HIFU focus at a depth of 12 mm within the sample, a removable “pointer” was attached to the transducer before each exposure. The pointer was also used to position the ultrasound imaging probe so that the HIFU axis was aligned with the B-mode imaging plane. After exposures, the tissue was sectioned and photographed to observe the lesion morphology.

C. Determination of *in situ* HIFU fields in gel phantoms and in tissue samples

For gel phantoms, a fiber-optic probe hydrophone of $100 \mu\text{m}$ diameter and 100 MHz bandwidth (FOPH 2000, RP

Acoustics, Leutenbach, Germany) was embedded at the depth of the HIFU focus in the gel before polymerization. Pressure waveforms were measured at increasing source power levels at the spatial maximum of the peak positive pressure. Measured waveforms were deconvolved using the FOPH impulse response provided by the manufacturer and the sensitivity of the FOPH was corrected to account for the slightly different acoustical properties of gel as compared to water.¹¹

In addition, our previous work demonstrated that HIFU shock waves with amplitudes of $40\text{--}80 \text{ MPa}$ measured by the FOPH may be underestimated by more than 25% due to the limited bandwidth of the hydrophone.¹¹ As this underestimation can significantly affect the calculation of the *in situ* heating rate, experimentally obtained waveforms were further corrected in the present work using numerical modeling.¹⁰ The measured waveforms were first compared to the previously modeled waveforms to ensure that the characteristics of the transducer did not change. In this step, the measured and modeled waveforms were compared at low levels of excitation ($p_0 < 0.3 \text{ MPa}$ for the 2 MHz source) to verify that they were equivalent. Then, at higher levels of excitation, when shocks were present, it was verified that only the peak positive pressures were different. The results of direct numerical modeling of nonlinear HIFU fields in the gel obtained in our previous study were then used to calculate heat deposition rates.^{11,18}

For bovine heart tissue, the *in situ* focal waveforms were measured at gradually increasing output levels behind a 12-mm -thick sample, which corresponded to the depth of the focus during HIFU exposures.¹⁰ The FOPH sensing tip was positioned at a distance of less than 1 mm from the distal surface of the tissue to ensure that propagation within the high-amplitude focal zone was predominantly through the tissue. Examples of the resulting experimental waveforms after deconvolution are shown as the thick curves in Fig. 2.

The measured waveforms were also corrected via modeling to compensate for underestimation of the peak positive pressure and the shock amplitude caused by the limited bandwidth of the hydrophone. In this step, a nonlinear derating method was used for estimation of focal waveforms in absorptive tissue using the existing results of nonlinear modeling in water.^{10,14}

In this previously developed method, a Khokhlov-Zabolotskaya-Kuznetsov (KZK) numerical model was calibrated versus free-field measurements and then used to simulate nonlinear HIFU fields in water. These results were “derated” to tissue to account for the greater attenuation of ultrasound in tissue versus water, whereas all other acoustic properties were assumed to be equal.^{11,14} This method is useful for HIFU fields because for highly focused transducers ($f\text{-number} \leq 1$, as is the case in the current study), the focal region of high pressures is significantly smaller than the focal distance. As nonlinear propagation effects are amplitude dependent, they dominate only near the focus and can be neglected in the prefocal region. Although this method does not account for the difference in the absorption of harmonics between water and tissue in the focal region, an error of only 5% is expected to result when predicting focal pressures. However, because the nonlinear parameter

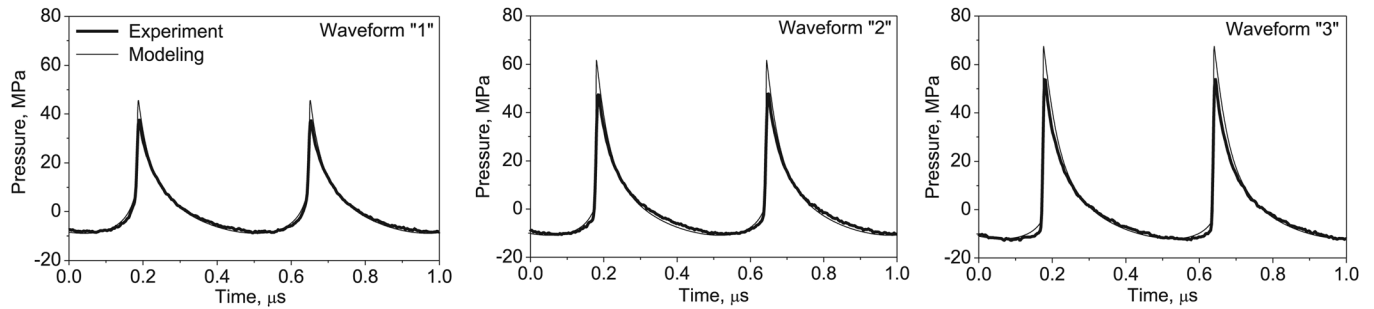


FIG. 2. *In situ* HIFU waveforms at different power outputs, modeled (thin line) and measured by the FOPH behind a 12-mm-thick layer of bovine heart tissue (thick line). The corresponding intensity and power levels are listed in Table I (exposures 1, 2, and 3 in the heart). High amplitude shock fronts are evident in the waveforms at higher outputs (2 and 3). The pressure waveform is distorted at the lowest output power used in this study but shocks are not fully developed (1).

is higher in tissue, the waveforms derated from water to tissue are less distorted by nonlinear effects than those measured in tissue.¹⁰ Here, we have extended the derating method to account for differences in both attenuation and nonlinearity between water and tissue.

In bovine liver, sonications were performed using 1.06, 2.158, and 3.42 MHz transducers. The transducers were operated to produce approximately the same peak positive and negative pressure levels in water as measured with the FOPH. For the 2 MHz transducer, the corresponding power setting was the same as for exposure 3, shown in Table I. The equivalent *in situ* pressure level for each transducer was generated by varying the depth of focus location within the tissue to account for the increase in attenuation with frequency; therefore, the focus was positioned 20, 12, and 6 mm below the tissue surface for the 1, 2, and 3 MHz transducers.

D. Nonlinear derating method to translate nonlinear HIFU fields from water to tissue

The method for derating nonlinear HIFU fields from water to tissue used in this work consists of three steps. In the first two steps, the attenuation coefficient and nonlinear parameter of the tissue were determined. In the last step, the focal waveform in tissue at higher output levels, when

shocks were present, was determined by derating numerical modeling results in water using the results of the first two steps. More detailed descriptions of each step of the refined derating method are provided in the following.

1. Determination of the attenuation parameter α in tissue

In the first step, focal waveforms were measured at low focal pressure amplitudes (2–3 MPa) less than 1 mm behind tissue samples of thickness equal to the focal depth $l = 12$ mm in subsequent HIFU exposures. The output level for these initial measurements was chosen so that acoustic propagation was purely linear, i.e., there was no harmonic content in the measured focal waveform. The measurements obtained behind the sample were then matched to the results of free-field modeling in water at lower outputs so that the focal waveforms were equivalent in amplitude in both cases. Simulations were performed using the KZK-type numerical model that was calibrated versus free-field measurements in our previous work.¹¹ Given the focal depth in tissue l , the attenuation parameter α at the HIFU frequency was determined from the ratio of the initial electric power of the source in tissue measurements and in water:

$$W_{el}(\text{water}) = W_{el}(\text{tissue}) \exp(-2\alpha l). \quad (1)$$

TABLE I. Summary of exposure parameters in gel and in bovine heart tissue.^a

Number	$p_{in\ situ}^+$ (MPa)	$p_{in\ situ}^-$ (MPa)	p_0 (MPa)	I_L <i>in situ</i> (kW/cm ²)	W_{el} (W)	t_{pulse} (ms)	PRF (Hz)	DF ^b	t_b (ms)
Polyacrylamide gel phantom									
	76	13.5	0.57	19.5	250	10	1	0.01	3.8
Bovine heart tissue									
1	45	9.0	0.37	7.23	110	10	1	0.01	N/A
2	61	11.0	0.46	11.23	164	10	1	0.01	8.1
3	67	12.0	0.55	16	236	10	1	0.01	4.5
4	67	12.0	0.55	16	236	10	0.3–100	0.003–1	4.5
5	67	12.0	0.55	16	236	0.2–100	0.1–50	0.01	4.5

^aThe HIFU frequency was 2.158 MHz and the initial pressure at the surface of the transducer, p_0 , was estimated using low amplitude measurements and modeling (Ref. 11). The *in situ* peak intensity at the focus was calculated assuming linear propagation, I_L , as $I_L = (p_0^2/2\rho_0 c_0)G^2 \exp(-2\alpha_0 L)$, where $G = 48$ is the linear focusing gain of the transducer in water, α_0 is ultrasound attenuation coefficient, and L is depth of the focus in tissue. *In situ* values for peak compression and peak rarefaction pressures, p^+ and p^- , were determined from the measured waveforms and corrected *via* modeling to compensate for the limited bandwidth of the FOPH (Ref. 10).

^bDuty factor.

Here, the electric power $W_{ei}(\text{water})$ corresponds to the initial pressure amplitude $p_0(\text{water})$ in the modeling that provides the same focal pressure amplitude. The attenuation parameter α at the HIFU frequency was 0.13 ± 0.03 Np/cm. This result is averaged over three different tissue samples.

2. Determination of the nonlinear parameter β in tissue

In the second step, focal waveforms were measured behind the same tissue sample at moderate outputs at which several harmonics (10–15) were present in the waveform and the bandwidth of the FOPH hydrophone was sufficient to capture the degree of the waveform distortion (Fig. 2, waveform “1”). These waveforms were compared to the waveforms modeled in water with the initial pressure $p_0(\text{water})$ scaled using Eq. (1) to account for attenuation in tissue. According to the results of the previously developed derating method, the focal waveforms in water and in tissue would be the same if the nonlinear parameters of these two media were the same. But, as the nonlinear parameter is higher in tissue, the waveform is steeper and has more energy at higher harmonics than that in water.¹¹

To compensate for the difference in nonlinearity between water and tissue, the following procedure was applied. As the degree of nonlinear effects in the KZK model in a nonabsorptive medium is determined by the parameter $N = 2\pi f_0 \beta p_0 / c_0^3 \rho_0$, which is proportional to the product of the initial source pressure p_0 and nonlinear parameter β of the propagation medium, a change in the nonlinear parameter is therefore equivalent to an increase of the initial pressure amplitude.¹⁴ In other words, the dimensionless pressure waveform $p_F^{\text{water},\beta}(t)/p_0$ at the focus in water with nonlinear parameter β will be the same as the waveform $p_F^{\text{water},\beta^*}(t)/p_0^*$ in water-like medium with tissue nonlinearity β^* if $\beta p_0 = \beta^* p_0^*$. The pressure input to the model $p_0^*(\text{water})$ thus was varied to find the best match to the nonlinear distortion of the measured waveform in tissue. Once this initial pressure was determined, then the nonlinear parameter of tissue β^* was calculated as

$$\beta^* = \beta p_0^* / p_0. \quad (2)$$

The degree of nonlinear distortion was also quantified by comparing the harmonic content of the measured and modeled waveforms, as shown in Fig. 3. In our work in bovine heart tissue, the best match was found when a value of $\beta^* = 4 \pm 0.1$ was used (equivalent nonlinear parameter, $B/A = 6$).

3. Determination of *in situ* focal waveforms with shocks from modeling in water

At higher outputs, when shocks were present, the calculated focal waveforms in water that corresponded to the *in situ* pressure waveform were obtained using the results of steps (1) and (2). The results of simulations in water for the initial pressure

$$p_0^*(\text{water}) = p_0(\text{water})\beta^* / \beta, \quad (3)$$

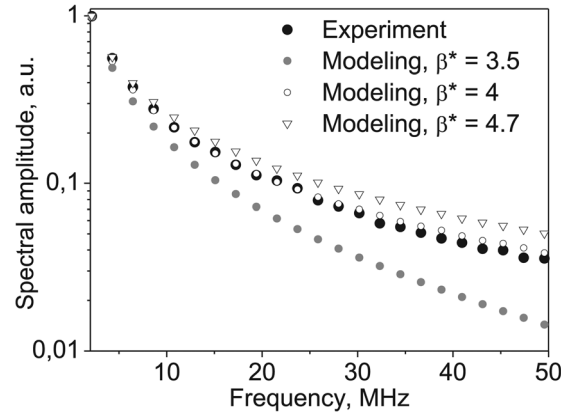


FIG. 3. Determination of the nonlinear parameter β^* in *ex vivo* heart tissue samples by comparing the spectra of the focal waveform measured in tissue (black dots) and derated from the modeling. The spectra correspond to the waveform 1 shown in Fig. 2. The best match was obtained when using $\beta^* = 4$.

were taken; then the pressure waveform at the focus equivalent to the waveform in tissue was calculated from the modeling results as

$$p_{F,\text{tissue}}(t) = p_{F,\text{water}}^*(t)\beta / \beta^*. \quad (4)$$

These modeled waveforms were compared to the measurements taken behind the sample and are shown in Fig. 2 (waveforms “2” and “3”). The shock amplitudes for calculating the boiling onset time were then determined from the modeled waveforms, Eq. (4), using the same methods described previously.¹⁰

E. Calculation of the time-to-boil

To establish a treatment protocol, theoretical calculations were performed to estimate the time to initiate boiling at the focus of the HIFU source. When high amplitude shocks are present at the focus, the absorption of ultrasound energy at the shocks becomes a dominant mechanism of tissue heating that increases the heating rate up to ~ 10 – 100 times greater than absorption at the fundamental frequency.¹⁰ The heating rate induced by an ultrasound wave containing shocks in the propagation medium can be calculated using weak shock theory¹⁹:

$$H = \frac{\beta f_0 A_s^3}{6\rho_0^2 c_0^4}, \quad (5)$$

where H is the heating rate, A_s is the *in situ* shock amplitude, β is the coefficient of nonlinearity, f_0 is the ultrasound frequency, c_0 is the ambient sound speed, and ρ_0 is the density of the medium. If the heating rate is large enough so that temperatures of 100°C are reached in tens of milliseconds, heat diffusion has little effect and can be neglected,¹⁰ therefore, the time-to-boil can be estimated as:

$$t_b = \frac{\Delta T c_v}{H}, \quad (6)$$

where ΔT is the change from the ambient temperature to 100 °C and c_v is the heat capacity per unit volume. The following physical constants were used for calculating time-to-boil in the gel phantom: $\rho_0 = 1044 \text{ kg/m}^3$, $c_0 = 1544 \text{ m/s}$, $\beta = 4.0$, $c_v = 5.3 \times 10^6 \text{ J m}^{-3} \text{ }^\circ\text{C}^{-1}$.¹⁸ The same parameters were used for estimations in heart and liver, as they reasonably fit characteristic values in soft tissue.²⁰

F. HIFU exposure parameters in gel and tissue samples

Sonications in gel and bovine heart were performed using the 2.158 MHz transducer. The exposure parameters varied over a wide range of power outputs, pulse durations, and duty factors. Several sets of experiments were performed in which one parameter was varied while keeping all others constant. The one parameter that was kept constant in all experiments was the total HIFU “on time” per exposure, which was 500 ms. This is a typical duration for “short” HIFU exposures, at which boiling temperatures are not expected to be reached assuming linear propagation conditions. The HIFU exposure parameters used in gel and heart tissue experiments are shown in Table I.

Sonications in bovine liver tissue were performed using 1.06, 2.158, and 3.42 MHz transducers. The output levels of the transducers were chosen to generate the same pressure levels at the focus *in situ* (Sec. II C). For the 2.158 MHz transducer, the *in situ* peak pressures corresponded to $p_0 = 0.57 \text{ MPa}$ and were known from our previous work: the peak positive pressure was 74 MPa and the peak negative pressure was 13 MPa (similar to exposure 3, Table I).¹¹ As explained in Sec. II C, the *in situ* levels for the 1.06 and 3.42 MHz transducers were approximately the same. The corresponding times to reach boiling in bovine liver tissue at each frequency, according to Eq. (6), were 5.6, 3.3, and 2.1 ms. Although the *in situ* pressures amplitudes were almost the same for each frequency, the boiling times decreased with frequency because within a given pulse duration, there were more acoustic cycles [Eq. (5)].

III. RESULTS

A. Mechanical lesions in transparent gel

Images and observations were made of the HIFU focus in gels with the high-speed camera and B-mode ultrasound. The parameters of HIFU exposures were the same in all experiments in gel and are listed in Table I. The time-to-boil calculated from the *in situ* shock amplitude was 3.8 ms, the pulse duration was 10 ms (which was approximately twice the time to boil), and the time between pulses was 1.0 s (DF = 0.01).

Figure 4 shows a sequence of images obtained during the first (left column) and the fifth (right column) pulses. Time $t=0$ corresponds to the arrival of each pulse. Both pulses induced cavitation, boiling, and similar bubble dynamics in the gels. At 1.2 ms, an optical effect of heating in the focal region is visible in Fig. 4 for both pulses as a dark elliptical region in the gel; subsequently, a large bubble fills the millimeter-sized width of this heated focal region. On

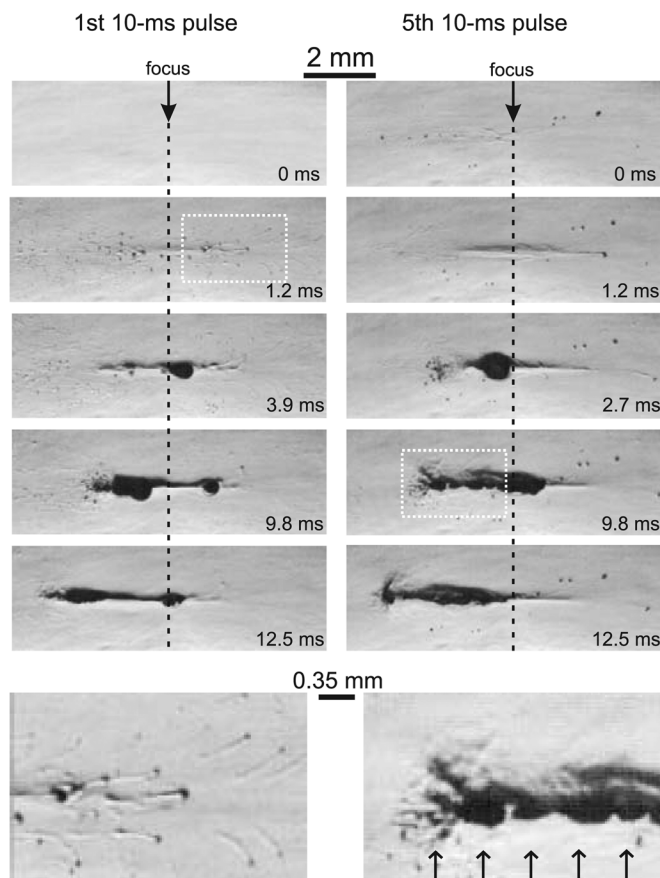


FIG. 4. High-speed images of HIFU pulsing in a transparent 7% BSA polyacrylamide gel during the first (on the left) and fifth (on the right) pulses. The frames were recorded at 20 000 frames per second (fps) with a $4 \mu\text{s}$ shutter speed; the frame taken at 0 ms corresponds to the start of each pulse. The HIFU source was on the left. The exposure parameters were: 2.158 MHz HIFU frequency, 10 ms pulse length, 1 Hz pulse repetition rate (PRF), $p^+ = 76 \text{ MPa}$ and $p^- = 13.5 \text{ MPa}$ (Table I). The start of boiling within each pulse is evident by the large millimeter-sized bubble that appears at the focus after 3.9 ms in the first pulse and in 2.7 ms in the fifth pulse. The shorter boiling time in the fifth pulse is likely due to an increased ambient temperature from the applied pulses relative to the first pulse. The images in the bottom row are enlarged versions of the white boxes that show cavitation bubbles moving through and beyond the focus (left) and a multi-layered cavitation bubble cloud forming in front of the boiling bubble due to reflection of the shock wave from the bubble surface (right). Bubble layers are spaced at approximately half the HIFU wavelength (0.35 mm) as indicated by the arrows at the bottom of the frame (Ref. 24).

the first pulse, this bubble appeared at 3.9 ms, which corresponded to the calculated time to boiling and is hereafter referred to as the boiling bubble. During the next several milliseconds of the HIFU pulse, two oscillating boiling bubbles were observed on both sides of the focus within the millimeter-sized heated region.

Using this pulsing scheme, boiling occurred within every pulse and the boiling bubble was not visible at the start of the next successive pulse. The time-to-boil decreased with successive pulses and was 2.7 ms in the fifth pulse as shown. The shorter time-to-boil for the fifth pulse as compared to the first was likely due to an accumulation of heat between pulses. During the rest of the pulsed exposure, boiling was initiated within each pulse at about the same time of 2–3 milliseconds and consistently started very close ($<1 \text{ mm}$) to the focus.

Micron-sized cavitation bubbles appeared in the first frame following the first pulse arrival, persisted throughout each exposure, and disappeared between pulses. Disappearance occurred during successive frames following the exposure. Cavitation bubbles were initially dispersed in a broad primarily prefocal region (1.2 ms) and were pushed by radiation force through and beyond the focus, as highlighted in the enlarged image. Although we have observed previously that visible smaller bubbles ($<100 \mu\text{m}$) can initiate slightly faster boiling, the movement of these bubbles is generally out of the focal region and the appearance of fewer bubbles with subsequent pulses as compared to the first pulse leads us to believe that the accelerated boiling with later pulses is primarily due to a buildup of heat and not to the presence of more nuclei from either inertial cavitation or boiling residuals. Previous calculations of thermal diffusion from the focal volume support this idea and show that the temperature does not return to ambient between pulses. Similarly, as bubbles are observed to be removed from the focus, we do not observe evidence of cavitation-enhanced heating leading to accelerated boiling.^{21,22}

Formation of a bubble cloud in front of the boiling bubble is observed in the frame taken at 2.7 ms of the fifth pulse and evenly spaced multiple layers of bubble clouds are clearly seen in the frame recorded at 9.8 ms close to the end of the pulse. As has been recently shown, these multilayered clouds are caused by the reflection of the shock wave from the surface of a millimeter-sized bubble.^{23,24}

Although cavitation bubbles distributed throughout the focal volume and localized boiling were both present in each pulse, emulsification of the gel followed the growth of the boiling bubble. Bubble activity and evolution of an eroded volume in the gel are shown in Fig. 5. High-speed images were taken at 9.5 ms of each 10 ms pulse (left column) and 1 s after each pulse, immediately prior to the subsequent pulse (right column). The residual damage of gel includes bubbles that can be seen in the images in the right column as dark spots, and the disruption of the polymer structure of the gel. The latter is hard to visualize, as illustrated by the bottom image in Fig. 5; therefore, in all other frames the areas of damage are outlined with a thin black line. No evidence of thermal denaturation, which would manifest itself as a hazy gray region, was present in the gels after HIFU sonication.

In the first pulse, although the boiling bubble originates from the focus of the transducer (Fig. 4), the two major areas of bubble motion are behind and in front of the focus, as shown by the dark areas in the left column. This motion produces two disruption areas that merge after several pulses. After 5 pulses, the range of bubble motion increases, and acquires more of a tadpole shape: the area in front (the “head”) is wider than the “tail” behind the focus. The residual damaged area (right column) enlarges in the same fashion as the bubble motion range. After 5 pulses, the length of the head of the lesion reaches its maximum size and does not change during the rest of the exposure. However, the width of the lesion and the length of the tail continue to grow. After 30 pulses, more residual bubbles are observed next to and behind the lesion, likely pushed from the focus by radiation pressure and collected in the postfocal region and at the pe-

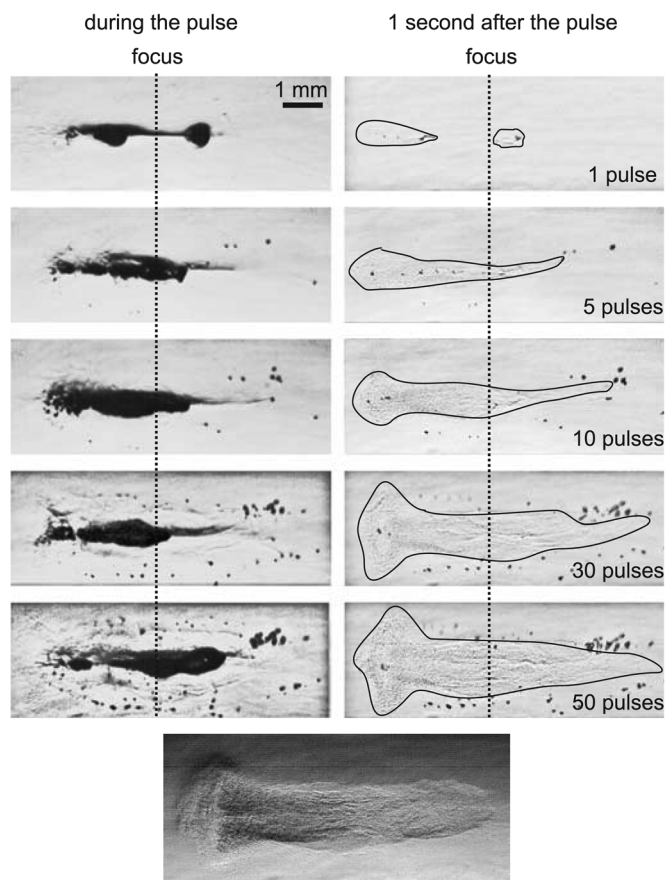


FIG. 5. High-speed camera images of lesion evolution in a polyacrylamide gel during pulsed HIFU exposures with 10 ms pulses and a 0.01 duty factor (same parameters as in Fig. 2). Images were recorded at 9.5 ms of each 10 ms pulse (left column) and 1 s after each pulse, immediately prior to the subsequent pulse (right column). A large boiling bubble forms during each 10 ms pulse (as shown in Fig. 2), but dissolves in the one second interval between pulses. Several smaller (tens of microns) residual bubbles remain between pulses and are evident in the frames on the right. These bubbles are largely pushed beyond the focus and away from the acoustic axis by the start of the subsequent pulse, collecting at the periphery of the lesion. The residual void of eroded gel is outlined in the right column for better visibility. Explosive growth of the bubble itself and also generation of high negative pressures caused by reflection of the shock wave from the bubble can contribute to tearing of the gel and lesion growth. The images were enhanced by zooming and altering the lighting to enhance the appearance of the residual void (bottom image), which contained gel pieces and infiltrated liquid and was no longer intact gel.

riphery of the lesion. Throughout the rest of the exposure, the damaged region broadens more uniformly; however, the maximum width of the head of the lesion does not change. The picture shown on the bottom of Fig. 5 is of another lesion in gel obtained with the same HIFU exposure parameters in which the residual disruption can be seen more clearly due to altered lighting. It is clear from this image that the polymer structure is disrupted; however, again, no evidence of thermal denaturation of the BSA protein in the phantom was present.

Figure 6 shows observations of bubble behavior during pulsed HIFU exposures by B-mode ultrasound and high-speed filming. The B-mode image taken immediately after the first HIFU pulse (first frame after HIFU was OFF) is shown in Fig. 6(a). The inset shows the corresponding region of the high-speed camera frame taken at 10 ms and depicts

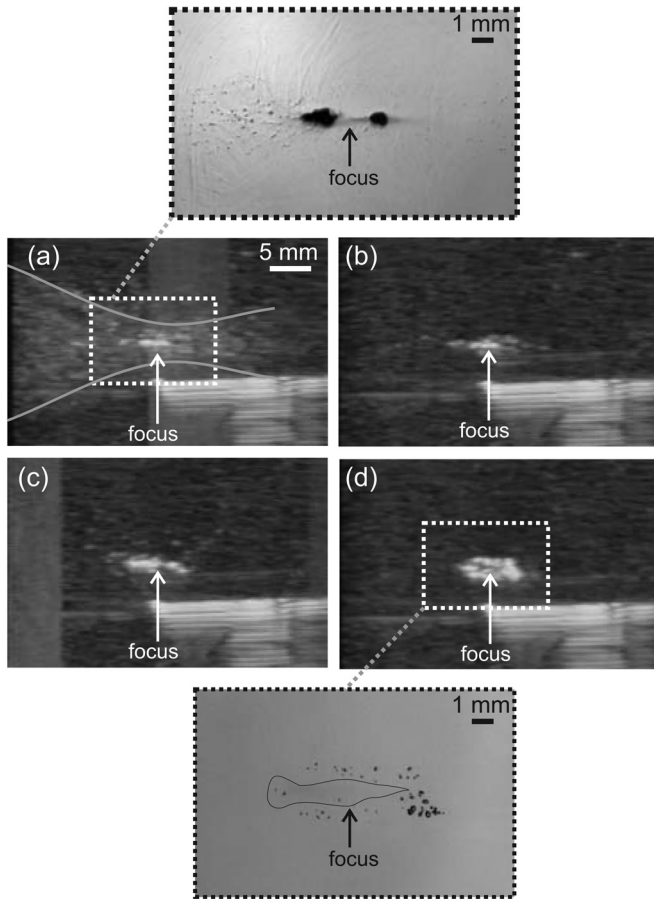


FIG. 6. B-mode images in a gel phantom at different time points during a pulsed exposure with the same parameters as used in Figs. 4 and 5: (a) 40 ms after the first pulse; (b) immediately prior to the second pulse; (c) 40 ms after the 10th pulse; (d) 40 ms after the 50th pulse. The needle in the lower right corner of the images was used for alignment purposes. A larger scale photo inset on the top (a) was taken at 10 ms and corresponds to the very end of the first HIFU pulse. The image shows the boiling bubbles at the focus and cavitation bubbles scattered throughout the hour-glass shape of the beam that creates a slight echogenicity on B-mode images but which disappeared shortly after the pulse (within 100–400 ms). Although no large boiling bubbles were evident between HIFU pulses in Fig. 3, the B-mode images showed a persistent echogenic region that continued to grow over 50 pulses (b–d). The second photo inset (on the bottom) confirms that the source of persistent echogenicity is the remnants of boiling bubbles pushed to the back and to the sides of the focus. The residual void is outlined for better visibility.

the very end of boiling. The hyperechoic line seen in the lower right-hand corner is the needle that was used for alignment purposes. A bright hyperechoic region at the focus of the transducer corresponded to the large (millimeter-sized) boiling bubble on the high-speed camera image. Faint spots of echogenicity are also scattered within the prefocal and, to some extent, postfocal region, as outlined by the thin gray curves. These correspond to small ($<100 \mu\text{m}$) cavitation bubbles, seen in the same region on the high-speed camera image. Cavitation bubbles disappeared very rapidly (in less than 3–4 B-mode frames or 150 ms) after HIFU was turned off and were not visible in the B-mode image of the sample right before the second pulse arrived, i.e., 1 s after HIFU was turned off [Fig. 6(b)]. However, the bright echogenicity from the boiling bubble persisted, indicating that the remnants of the boiling bubble in the lesion cavity did not fully dissipate

before the next pulse arrived. Also, the remnants appeared much brighter on B-mode images than cavitation bubbles observed during the HIFU pulse, presumably due to the slow frame rate of the ultrasound imager (24 frames/s). Although cavitation bubbles created during HIFU irradiation (top frame in Fig. 6) were observed to grow up to the same size as boiling bubble remnants after HIFU was turned off (bottom frame in Fig. 6), they did not produce the same level of echogenicity. Presumably, the growth and collapse of cavitation bubbles (which occurs on the order of a single acoustic cycle), was much shorter than the frame rate of the imager. On the contrary, after HIFU was turned off, residual boiling bubbles persisted and shrank slowly (on a time scale of tens to hundreds of milliseconds), thus their visibility on B-mode images was not affected as much by temporal averaging.

In Figs. 6(c) and 6(d), B-mode images of the same sample after 10 and 50 pulses of HIFU are shown. The length of the echogenic region does not change considerably; however, the width increases with the number of pulses. This observation agrees well with the high-speed camera recordings shown in Fig. 5. The inset in Fig. 6(d) shows the corresponding high-speed camera frame of the gel 80 ms after applying 50 pulses of HIFU. Residual bubbles can be clearly observed around the focal area that, according to Fig. 5, is most likely a void filled with gel remnants and infiltrated liquid. The structure of the echogenicity in the B-mode image repeats the distribution of the residual bubbles surrounding the void; the void itself is seen as a darker region between two echogenic layers of bubbles.

B. Emulsified lesions in *ex vivo* heart tissue

The results of sonications in *ex vivo* bovine heart with the same HIFU exposure parameters as in the experiments with gel phantoms [pulse length 10 ms, pulse repetition rate (PRF) 1 Hz, 50 pulses—exposure 3 in Table I] resulted in boiling within each pulse and localized tissue emulsification as seen in Fig. 7. An example of the B-mode image series during this exposure is shown in Fig. 7(a) to compare with the B-mode ultrasound observations recorded in gels. The images represent the B-mode frames before HIFU exposure and the first frames after the 1st, 12th, and 33rd HIFU pulses. As observed in the gel experiments, an echogenic region from boiling appears in images during each pulse, starting from the very first pulse. However, the echogenic region in tissue is not as evident as in gel, likely because of increased signal from the surrounding tissue structure, which is less homogeneous than the gel phantoms. Similar to the gel experiments, the width of the hyperechoic region grows with increasing number of pulses. The echogenic region first originates at the focus, where heating is the greatest, and then shifts slightly ($\sim 1 \text{ mm}$) toward the transducer. Unlike the results of gel experiments, pre-focal cavitation bubbles were not evident in the images. The remnants of boiling bubbles that created echogenicity between HIFU pulses disappeared faster than in gel. No echogenicity was observed *prior* to the arrival of the next pulse within the first ten pulses of exposure. With an increasing number of pulses the echogenicity was observed to persist for longer time periods; it was

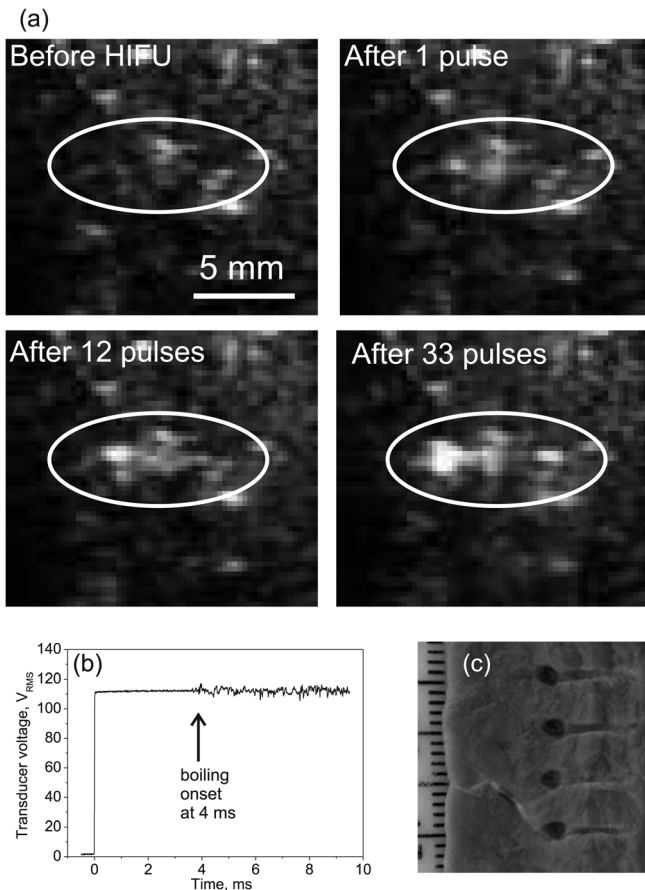


FIG. 7. (a) Selected frames of ultrasound B-mode images of *ex vivo* bovine heart tissue recorded during pulsed HIFU sonication (exposure 3 in Table I). Similar to images in gel (Fig. 6), echogenicity in tissue appears with the very first pulse as boiling bubbles are induced by HIFU. (b) Recording of the transducer voltage during the first pulse of exposure gives further evidence that bubble activity is specifically boiling: fluctuations in the signal occurred at 4 ms during the 10 ms pulse, in agreement with theoretical estimations of the time-to-boil. (c) The lesions produced by four consecutive exposures were voids that were almost identical in size and shape, filled with liquefied tissue (evacuated from the voids in the photo), with no visible signs of thermal denature. The tadpole shape of the lesions was similar to the echogenic region observed in B-mode images (a).

present between pulses starting from about the 10th pulse and remained up to 10–20 s after the 50th pulse.

The onset of boiling in these experiments was determined within each pulse from the HIFU source drive voltage. An example of a typical voltage signal recorded during HIFU pulsing is shown in Fig. 7(b). The start of voltage fluctuations (in this particular case in 4 ms) indicated the start of boiling. The time to onset of voltage fluctuations varied slightly from sample to sample (3.7 ± 0.9 ms), but corresponded well with theoretical predictions performed using Eqs. (5) and (6). Each exposure resulted in a volume of emulsified tissue as shown in Fig. 7(c). The emulsified volumes had repeatable locations, sizes, and tadpole shapes. The position of the transducer focus corresponded to the junction between the round head and narrow tail of the lesion. This observation corresponds well to the high-speed images of lesion development recorded in gels (Fig. 5): the region of bubble activity expands toward the transducer, forming the wide head of the lesion. The length of the lesion

is 8 mm for both the heart tissue and gel, and the width of the tail is also similar (1 mm). However, the maximum width of the head of the lesion is somewhat larger in tissue (2.5 mm) than in gel (1.5 mm).

C. Effect of HIFU exposure parameters on mechanical and thermal effects in tissue

Further experiments were performed with modified HIFU pulsing schemes to study how various degrees of thermal or mechanical bioeffects occur in tissue and to test whether boiling was necessary to induce tissue emulsification. Changes were made to the HIFU pulsing scheme by varying the pulse duration, the duty factor, and the focal pressures.

1. Pulse duration and duty factor

The heart tissue was sonicated with a total HIFU ON duration of 500 ms and constant power to the HIFU source corresponding to waveform 3 in Fig. 2. When the pulse duration was varied from 0.2 to 100 ms (~ 0.05 – $30 t_b$), the total time of exposure was 50 s and the PRF was adjusted to maintain a duty factor of 0.01 (Table I, exposure 5). Likewise, when the duty factor was changed within the range 0.003–1, the pulse duration of 10 ms was kept constant (Table I, exposure 4).

The resulting lesions were classified into three different types that are illustrated in Fig. 8. The photos in Figs. 8(a) and 8(b) were taken with the lesion content preserved (top images) and removed (bottom images). The lesion shown in Fig. 8(a) is of a cavity filled with liquid that is the same color as unaffected tissue and which can be easily removed. No apparent thermal denaturation (visible as a change in color to white) was observed. This type of lesion was therefore categorized as purely mechanical emulsification of tissue. Figure 8(b) shows a lesion with mixed mechanical and

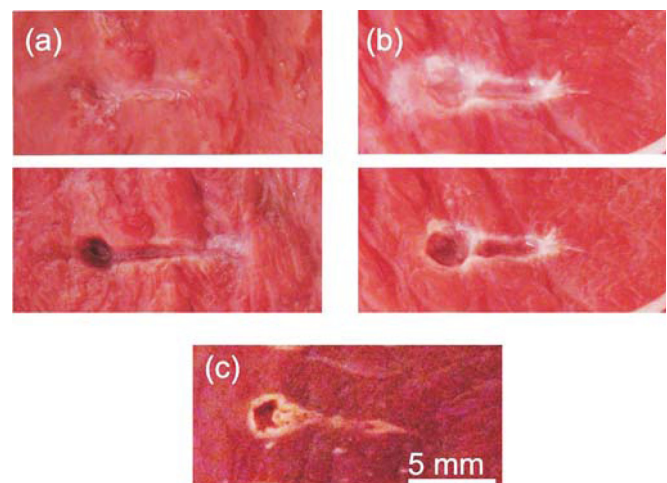


FIG. 8. (Color online) Types of lesions produced by different HIFU pulsing schemes in *ex vivo* bovine heart tissue. (a) Type 1: void with no signs of thermal damage filled with liquefied tissue (top photo) that can be poured out (bottom photo). With an increase of pulse duration and/or duty factor, the lesion transforms into (b) type 2: void with coagulated edges, filled with white paste (top photo), that can be easily removed (bottom photo). With a further increase in pulse duration and/or duty factor, the result is (c) type 3: a solid thermal lesion with an evaporated core.

thermal damage. The edges of the lesion appear white, which indicates thermal denaturation of tissue. The lesion is filled with white paste that can also be easily removed. The third type of lesion, represented in Fig. 8(c), is a solid thermal lesion with a vaporized core. It also has a tadpole shape, with a larger cavity at the head and a smaller one at the tail, which are formed by boiling bubble activity. This classification is very similar to that used to categorize lesions resulting from different histotripsy protocols.⁴

Table II summarizes the effects of pulse duration and duty factor on the lesion type. Thermal effects become more pronounced as the pulse duration or the duty factor increase. Purely mechanical damage was achieved only with duty factors of less than 0.02 and pulse durations of less than 30 ms (10 times the time-to-boil in this case). Purely thermal damage occurred for pulse lengths longer than 100 ms or duty factors larger than 0.02. All of the cases in between can be referred to as mechanical damage with varying degrees of thermal effects. These lesions can all be referred to as type two, with a variable extent of border denaturation and paste thickness.

2. HIFU transducer power

In these experiments, the power to the source was varied so that the focal waveform shape changed from being nonlinearly distorted (waveform 1 in Fig. 2) to forming a high amplitude shock wave (waveforms 2 and 3 in Fig. 2). All other exposure parameters were kept constant and are listed in Table I under exposures 1–3. Figure 9 displays the results of this experiment. Tissue emulsification was observed and boiling was detected by power fluctuations and B-mode ultrasound at all of the source power levels except for the case of waveform 1. The pressure waveform was distorted by nonlinear propagation effects, but the shock front was not fully developed in waveform 1, i.e., the pressure change within the 10 ns interval associated with a shock measured by the FOPH of 100 MHz bandwidth was much smaller than the peak positive pressure in the waveform.¹⁰ The heating rate was insufficient to initiate boiling within each pulse, and no obvious lesion was produced. When outputs were higher (waveforms 2 and 3 in Fig. 2), each pulse was long enough to induce boiling and emulsified lesions were obtained. The peak negative pressure changed only slightly between exposures 1 and 2; therefore, cavitation was minimally altered, yet the liquefied

TABLE II. Effect of pulse duration and duty factor on the type of lesion produced in *ex vivo* heart samples: type 1—void filled with liquefied tissue with no signs of thermal denaturation in the filling or tissue surrounding the void; type 2—void with coagulated edges, filled with white paste that represents partially coagulated, emulsified tissue; type 3—solid thermal lesion with a vaporized core.

Pulse duration (ms)	Duty factor	Duty factor			
		0.005	0.01–0.02	0.03–0.2	0.2–1
4–10	(1 – 3 t_b)	1	1	2	3
10–30	(3 – 10 t_b)	1	2	2	3
30–100	(10 – 30 t_b)	2	2	3	3
100–500	(> 30 t_b)	3	3	3	3

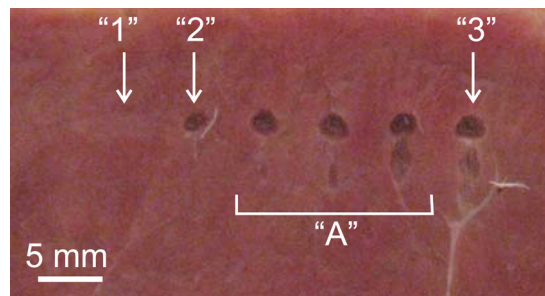


FIG. 9. (Color online) Cross section in the axial plane of lesions induced in bovine heart using 50 HIFU pulses of 10 ms duration, 1 Hz PRF, and increasing power to the HIFU source (from left to right). *In situ* HIFU waveforms for the lesions 1, 2, and 3 are shown in Fig. 1 and details of the exposure parameters are listed in Table I with the same numbering. No lesions were produced when the focal waveform corresponded to 1 (Fig. 2), as the heating rate was not sufficient to initiate boiling within each pulse as shocks were not yet formed at the focus. At higher outputs (cases 2, 3, and in between them grouped under “A”), shocks were present at the focus (see Fig. 1), boiling was induced within each pulse, and emulsified lesions were produced. The peak negative pressure changed only slightly between exposures 1, 2, and 3; therefore, cavitation activity was only minimally altered. The results from this experiment thus demonstrate that liquefied voids were only observed when shocks and boiling were present.

voids were only observed when shocks and boiling were present. There was no thermal denaturation observed at the transducer power levels used in these experiments.

3. HIFU frequency

The effect of HIFU frequency on the lesion shape and size was studied in *ex vivo* bovine liver samples. The exposure parameters at the focus were the same for all three exposures: the *in situ* focal pressure was $p^+ = 74$ MPa, $p^- = 13$ MPa, the duty factor was 0.01, and the total HIFU on time was 500 ms. The pulse duration used in all of these experiments was approximately three times longer than the time to initiate boiling for each frequency: 20 ms (1 MHz), 10 ms (2 MHz), and 5 ms (3 MHz). Representative lesions from these experiments are shown in Fig. 10.

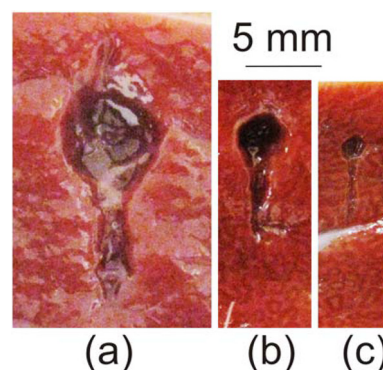


FIG. 10. (Color online) Axial cross-sections of liquefied lesions obtained in *ex vivo* bovine liver using HIFU transducers of the same geometry but operating at different frequencies: (a) 1.1 MHz, (b) 2.158 MHz, and (c) 3.4 MHz. To balance the comparison, the transducer f -number = 1, the *in situ* focal pressure ($p^+ = 74$ MPa, $p^- = 13$ MPa), duty factor (0.01), and total HIFU on time (500 ms) were the same for all three exposures. In addition, pulse lengths were approximately three times longer than the time-to-boil for each frequency: 20 ms, 10 ms and 5 ms, respectively. Larger lesions were obtained with lower frequencies and the total lesion size followed the dimensions of the heated focal region for each transducer.

All of the lesions are voids filled with liquefied tissue. The overall tadpole shape of the lesion did not change with frequency, and the lesion size was proportional to the size of the focal region of each transducer. The overall length of the lesion was inversely proportional to the frequency, which suggests that the length is determined by the axial length of the focal lobe of the beam. Detailed characterization of the acoustic field is available for the 2 MHz transducer from previous work.¹⁰ The length of the lesion for this frequency (8 mm) agrees very well with the length of the focal lobe (7 mm at -6 dB in a linear beam) where shock fronts were present and heat deposition is efficient. The width of the round head of the void is larger (3 mm) than the focal beam width of the 2 MHz transducer (1 mm at -6 dB in a linear beam). The round shape of the head suggests that its size is determined by the maximum expansion size of the boiling bubble, which increases throughout the exposure as the heated region broadens.

An interesting detail of the lesion shape is clearly observed at 1 MHz—a small cavity appears in front of the lesion facing the transducer. This cavity is smaller for the lesion created by the 2 MHz transducer, and though present, barely visible for the 3 MHz transducer. A similar “bump” at the head of the lesion was observed in the gel experiments (Fig. 5, bottom photo in the right column). The physical reason for this effect has not yet been investigated.

IV. DISCUSSION AND CONCLUSIONS

In this paper, a recently proposed method to induce mechanical damage in bulk tissue using high intensity focused ultrasound is examined. The general approach is to use millisecond-long pulse sequences of ultrasound waves that evolve into shocks and induce boiling in tissue within each pulse. The experiments performed in gel phantoms and *ex vivo* heart and liver tissue showed that mechanically emulsified lesions with no evident thermal damage can be induced using this method and varying degrees of thermal effects can be produced by varying the parameters of the pulsing scheme. Tissue emulsification was only observed for exposures where shocks were present in the pressure waveform at the HIFU focus, and only when boiling was initiated. As boiling bubbles are highly echogenic, tissue emulsification can be easily monitored in real-time using B-mode ultrasound imaging. Note that the presence of boiling alone is not sufficient to induce emulsification; high-amplitude shocks must be present to heat the tissue and to create a boiling bubble within tens of milliseconds. With lower amplitude waves, boiling temperatures are reached after much longer heating durations, in hundreds of milliseconds to several seconds, and a thermally necrotic volume appears before boiling starts. The result of these lower amplitude exposures with boiling is a solid thermal lesion with a vaporized core.¹⁷

Based on the previous observations that shock wave heating can lead to temperatures of 100 °C and tissue boiling within milliseconds,¹⁰ a protocol was chosen in which the pulse length was only slightly longer than the expected time-to-boil. When sufficient time was allowed between pulses for the tissue to cool, the damage induced was purely me-

chanical and contained no visible signs of thermal denaturation. If the duty factor was increased, i.e., the cooling time was decreased, or if the pulse length was considerably longer than the time-to-boil (>30 ms), then the lesion morphology changed and contained increasing amounts of thermal damage. No evident thermal effects were detected when using duty factors of less than 0.02 and pulse durations of less than 30 ms. Higher duty cycles or longer pulses produced a thick white paste with varying degrees of thermal denaturation.

No evidence of thermal denaturation in the emulsified lesions in the gels and in tissue were present, which may seem contradictory since temperatures at the focus were close to 100 °C. However, according to previous measurements, the region heated by shock waves is extremely localized (0.2 mm in width at 1/2 level).¹⁰ Thus, some amount of BSA protein in the gel or some volume of tissue may be denatured, but it was negligible compared to the volume of the resulting lesion and may only be detectable using more sensitive protein analysis methods, which were not employed here.

In previous studies on histotripsy, it was demonstrated that microsecond-long pulses of shock waves can produce purely mechanical tissue damage.⁴ The physical mechanism for this effect has been attributed to cavitation. The pulsing method proposed here to produce emulsification is different in that the acoustic pressures are about two times lower and the pulses are about 1000 times longer. The method relies on generating shock amplitudes of 40–80 MPa at the focus to produce enhanced heating rather than relying on generating very large negative pressures to produce cavitation clouds, as used in the histotripsy approach. Inertial cavitation, but not the densely populated bubble clouds seen in histotripsy, was also present in all of our exposures, as shown by high-speed images obtained in gels; however, emulsified lesions were obtained only when shocks and repetitive boiling were present. This reliance on heating was best demonstrated in experiments where the power to the HIFU source was varied from 110 to 236 W (exposures 1–3 in Table I). As the power was decreased, the shock amplitude and consequently the heating rate, decreased dramatically (Fig. 2), whereas the peak negative pressure, responsible for cavitation, was nearly unchanged and was always above the cavitation threshold of the gel phantoms.²⁵ When a shock front did not form (power setting 1 in Fig. 2) boiling was never initiated with the pulsing parameters used and tissue damage was not observed.

In multiple experiments, boiling bubbles were readily observed on B-mode ultrasound in gels and in tissue. Further, correlations between cavitation and boiling bubble activity were further studied by comparing high-speed images obtained in gel phantoms with simultaneous B-mode images. In gels, boiling bubbles appeared as bright and persistent echogenic regions, whereas cavitation bubbles appeared as dim and transient echogenic regions, and disappeared shortly after HIFU was turned off. When boiling was not initiated, bright hyperechoic regions were not observed. In tissue, boiling bubbles also appeared as bright echogenic regions, but cavitation was not sufficiently echogenic to be observed in inhomogeneous tissue. These findings have further

implications in ultrasound-guided HIFU. In several publications, the appearance of bright persistent echogenicity on B-mode ultrasound was interpreted as cavitation and was considered to be unrelated to thermal effects.^{26,27} Our results described herein suggest that the appearance of this type of echogenicity likely represents boiling, and thus implies heating of the tissue to 100 °C. In histotripsy studies, echogenicity was observed during treatments, but was associated with the evolution of a dense cavitation bubble cloud, which can only be initiated in bulk tissue at extremely high (>20 MPa) negative pressures.

The technique for mechanical tissue disruption presented herein relies on the ability to estimate the *in situ* time-to-boil. The time-to-boil can be consistently measured from the initiation of HIFU-source-voltage fluctuations *in vitro* and *ex vivo*.¹⁰ These measurements corresponded well to theoretical predictions based on weak shock theory and were repeatable in *ex vivo* tissue. The characterization data of a HIFU field in water and the application of nonlinear derating methods thus can provide a good estimation of the *in situ* shock wave amplitude and the time-to-boil, which was shown here to be within 1–2 ms from the measured one, i.e., 25% accuracy. B-mode ultrasound can also provide another means of measuring the time-to-boil. Short millisecond HIFU pulses can be sent at low PRF (~1 Hz), and the pulse duration can be gradually increased until echogenicity appears at the focus, which corresponds to the start of boiling. Once the time-to-boil is determined for a specific HIFU output and frequency, the extent of thermal effects and the size of the lesion can be controlled by choosing appropriate sonication parameters such as the PRF and pulse duration.

In cases when purely mechanical tissue destruction was induced in the present study, the contents of the lesion did not appear to have tissue remnants large enough to be seen by the naked eye (~100 μm). The residual liquid contained in the lesion appeared homogenous and had the same color as the undisturbed tissue. With an increase of the pulse duration and/or the duty factor, the lesion transformed into a void with coagulated edges, filled with white paste, and was not intact at the edges. A further increase in pulse duration and/or duty factor resulted in a solid thermal lesion with an evaporated core, which is typical for HIFU treatments using continuous exposures (>1 s) with boiling. In the future, more thorough analysis of the lesion contents could be performed, as has been done in histotripsy experiments.²⁸

The mechanisms of tissue emulsification using shock wave heating and millisecond boiling are yet to be understood. We propose here two mechanisms based on our experimental observations. One mechanism can be attributed to the explosive growth of a boiling bubble in superheated tissue (i.e., temperatures of greater than 100 °C before boiling initiation). We speculate that shear stress on tissue resulting from rapid bubble expansion may lead to rupture of connective tissue and cell membranes. The bubble cools down and stops growing once it becomes larger than the localized focal region heated by shocks. This is in agreement with observations as the head of the emulsified lesion is round and its size corresponds to the length of the focal zone of the HIFU beam where heating by shock waves occurs.

Besides boiling bubble expansion, the presence of shocks in combination with a millimeter-sized void at the focus, suggests another mechanism of mechanical tissue damage. As illustrated in Fig. 4, a multilayered cavitation bubble cloud forms in front of the boiling bubble. These bubbles are presumably initiated by very high negative pressures caused by reflection of shock waves from the free boundary of the bubble, conversion of high amplitude compressional peak pressures into rarefactional pressures and interference of this rarefaction phase of the incident wave with the incident pulse, first at a distance ~1/4 of a wavelength from the bubble interface and then every 1/2 of a wavelength. This effect has been observed previously in lithotripsy fields and the formation of multi-layer bubble clouds in HIFU fields has recently been reported.^{23,24} The formation of bubbles also may weaken the structure of the medium in front of the boiling bubble, allowing radiation force to tear the layer adjacent to the bubble and push pieces of gel or tissue into the cavity. Again, this mechanism is also limited to the region, where shocks and boiling bubbles are present.

The results obtained with the proposed millisecond-boiling method show significant potential for clinical HIFU applications. Voids in tissue were obtained with clinically relevant HIFU amplitudes and transducer dimensions and were repeatable in location and size. The method utilizes highly localized enhanced heating by shocks to resolve problems stemming from the stochastic nature of cavitation that is inherent in other methods of tissue emulsification. The presence of nuclei within the heated volume is still necessary to initiate boiling and therefore the tissue may be superheated before boiling starts. The possible superheating of tissue enhances energy concentration at the focus, and leads to the explosive growth of boiling bubbles and localized mechanical tissue damage.

The work presented herein demonstrates that shock wave heating and millisecond boiling offer an effective method for inducing mechanical emulsification in tissue with B-mode ultrasound guidance. The size of the lesions and degree of thermal effects can be predicted theoretically and controlled through the proper choice of HIFU frequency and pulsing scheme.

ACKNOWLEDGMENTS

This work was supported by the National Institutes of Health (EB007643 and DK007742), the National Space Biomedical Research Institute through NASA NCC 9-58, the Russian Foundation for Basic Research (09-02-01530), and the Acoustical Society of America through the Frederick V. Hunt Postdoctoral Research Fellowship in Acoustics. The authors gratefully acknowledge Francis Olson at APL for help in the design and construction of the experimental setup, Julianna Simon at APL for help with measurements, and Adam Maxwell at the University of Michigan for useful discussions.

¹C. R. Hill, J. C. Bamber, and G. ter Haar, *Physical Principles of Medical Ultrasonics*, 2nd ed. (Wiley, West Sussex, UK, 2004, Chap. 13.

²K. Hynynen and J. Souquet (Eds.), *29th International Symposium on Therapeutic Ultrasound*, Aix-en-Provence, September 24–26, 2009 (AIP Conference Proceedings. Vol. 1215, 2010), pp. 3–15, 88–110, 216–234.

- ³J. Tavakkoli, A. Birer, A. Arefiev, F. Prat, J. Chapelon, and D. Cathignol, "A piezocomposite shock wave generator with electronic focusing capability: application for producing cavitation-induced lesions in rabbit liver," *Ultrasound Med. Biol.* **23**(1), 107–115 (1997).
- ⁴J. Parsons, C. Cain, G. Abrams, and J. Fowlkes, "Pulsed cavitation ultrasound therapy for controlled tissue homogenization," *Ultrasound Med. Biol.* **32**(1), 115–129 (2006).
- ⁵T. L. Hall, C. R. Hempel, K. Wojno, Z. Xu, C. A. Cain, and W. W. Roberts, "Histotripsy of the prostate: dose effects in a chronic canine model," *Urology*. **74**(4), 932–937 (2009).
- ⁶N. Smith and K. Hynynen, "The feasibility of using focused ultrasound for transmyocardial revascularization," *Ultrasound Med. Biol.* **24**(7), 1045–1054 (1998).
- ⁷W. Roberts, T. Hall, K. Ives, J. Wolf, J. Fowlkes, and C. Cain, "Pulsed cavitation ultrasound: a noninvasive technology for controlled tissue ablation (histotripsy) in the rabbit kidney," *J. Urol.* **175**(2), 734–738 (2006).
- ⁸Z. Xu, T. Hall, J. Fowlkes, and C. Cain, "Effects of acoustic parameters on bubble cloud dynamics in ultrasound tissue erosion (histotripsy)," *J. Acoust. Soc. Am.* **122**(1), 229–236 (2007).
- ⁹M. Canney, V. Khokhlova, J. H. Hwang, T. Khokhlova, M. Bailey, and L. Crum, "Tissue erosion using shock wave heating and millisecond boiling in high intensity ultrasound field," in *Proceedings of the 9th International Symposium on Therapeutic Ultrasound, September 23–26, 2009, Aix-En-Provence, France*, pp. 36–39.
- ¹⁰M. Canney, V. Khokhlova, O. Bessonova, M. Bailey, and L. Crum, "Shock-induced heating and millisecond boiling in gels and tissue due to high intensity focused ultrasound," *Ultrasound Med. Biol.* **36**(2), 250–267 (2010).
- ¹¹M. Canney, V. Khokhlova, M. Bailey, O. Sapozhnikov, and L. Crum, "Acoustic characterization of high intensity focused ultrasound fields: A combined measurement and modeling approach," *J. Acoust. Soc. Am.* **124**(4), 2406–2420 (2008).
- ¹²G. Schatzl, W. Chen, R. Carlson, A. Lowe, N. Sanghvi, and M. Marberger, "Real-time monitoring of tissue changes during the treatment of prostate cancer with high intensity focused ultrasound (HIFU)," *J. Endourol.* **24**(S1), paper PS22-1 (2010).
- ¹³N. T. Sanghvi, F. J. Fry, R. Bihrl, R. S. Foster, M. H. Phillips, J. Syrus, A. Zaitsev, and C. Hennige, "Microbubbles during tissue treatment using high intensity focused ultrasound," *Proc. IEEE*, **2**, 1571–1574 (1995).
- ¹⁴O. Bessonova, V. Khokhlova, M. Bailey, M. Canney, and L. Crum, "A derating method for therapeutic applications of high intensity focused ultrasound," *Acoust. Phys.* **56**(2), 296–306 (2010).
- ¹⁵L. Crum and W. Law, "The relative roles of thermal and nonthermal effects in the use of high intensity focused ultrasound for the treatment of benign prostatic hyperplasia," *Proceedings of the 15th International Congress on Acoustics, Trondheim, Norway*, 1995, pp. 315–318.
- ¹⁶C. Thomas, C. Farny, T. Wu, R. Holt, and R. Roy, "Monitoring HIFU lesion formation in vitro via the driving voltage," in: *Therapeutic Ultrasound: 5th International Symposium on Therapeutic Ultrasound*, edited by G. Clement, N. McDannold, and K. Hynynen (American Institute of Physics, Melville, NY, 2006), pp. 293–297.
- ¹⁷T. Khokhlova, M. Canney, D. Lee, K. Marro, L. Crum, V. Khokhlova, and M. Bailey, "Magnetic resonance imaging of boiling induced by high intensity focused ultrasound," *J. Acoust. Soc. Am.* **125**, 2420–2431 (2009).
- ¹⁸C. Lafon, V. Zderic, M. Noble, J. Yuen, P. Kaczkowski, O. Sapozhnikov, F. Chavrier, L. Crum, and S. Vaezy, "Gel phantom for use in high-intensity focused ultrasound dosimetry," *Ultrasound Med. Biol.* **31**(10), 1383–1389 (2005).
- ¹⁹*Nonlinear Acoustics*, edited by M. Hamilton and D. Blackstock (Academic, London, 1998), Chap. 4, p. 106.
- ²⁰F. Duck, *Physical Properties of Tissue: A Comprehensive Reference Book* (Academic, London, 1990), pp. 9–137.
- ²¹C. C. Coussios, C. H. Farny, G. ter Haar, and R. A. Roy, "Role of acoustic cavitation in the delivery and monitoring of cancer treatment by high-intensity focused ultrasound (HIFU)," *Int. J. Hypertherm.* **23**(2), 105–120 (2007).
- ²²C. H. Farny, G. R. Holt, and R. A. Roy, "The correlation between bubble-enhanced HIFU heating and cavitation power," *IEEE Trans Biomed Eng.* **57**(1), 175–184 (2010).
- ²³Y. A. Pishchalnikov, J. A. McAteer, I. V. Pishchalnikova, J. C. Williams, Jr., M. R. Bailey, and O. A. Sapozhnikov, "Bubble proliferation in shock wave lithotripsy occurs during inertial collapse," *AIP Conf. Proc.* **1022**, 460–463 (2008).
- ²⁴A. D. Maxwell, T. Y. Wang, C. A. Cain, J. B. Fowlkes, Z. Xu, O. A. Sapozhnikov, and M. R. Bailey, "The role of compressional pressure in the formation of dense bubble clouds in histotripsy," in *Proceedings of the IEEE International Ultrasonics Symposium* (IEEE, Piscataway, NJ, 2009), pp. 81–84.
- ²⁵V. Khokhlova, M. Bailey, J. Reed, B. Cunitz, P. Kaczkowski, and L. Crum, "Effects of nonlinear propagation, cavitation, and boiling in lesion formation by high intensity focused ultrasound in a gel phantom," *J. Acoust. Soc. Am.* **119**(3), 1834–1848 (2006).
- ²⁶S. Vaezy, M. Andrew, P. Kaczkowski, and L. Crum, "Image-guided acoustic therapy," *Annu. Rev. Biomed. Eng.* **3**, 375–390 (2001).
- ²⁷B. Rabkin, V. Zderic, L. Crum, and S. Vaezy, "Biological and physical mechanisms of HIFU-induced hyperecho in ultrasound images," *Ultrasound Med. Biol.* **32**(11), 1721–1729 (2006).
- ²⁸Z. Xu, Z. Fan, T. Hall, F. Winterroth, J. Fowlkes, and C. Cain, "Size measurement of tissue debris particles generated from pulsed ultrasound cavitation therapy—histotripsy," *Ultrasound Med. Biol.* **35**(2), 245–255 (2009).